

Approximate Similarity Search for Online Multimedia Services on Distributed CPU–GPU Platforms

George Teodoro · Eduardo Valle · Nathan Mariano ·
Ricardo Torres · Wagner Meira Jr · Joel H. Saltz

Received: date / Accepted: date

Abstract Similarity search in high-dimensional spaces is a pivotal operation found a variety of database applications. Recently, there has been an increase interest in similarity search for online content-based multimedia services. Those services, however, introduce new challenges with respect to the very large volumes of data that have to be indexed/searched, and the need to minimize response times observed by the end-users. Additionally, those users dynamically interact with the systems creating fluctuating query request rates, requiring the search algorithm to adapt in order to better utilize the underline hardware to reduce response times. In order to address these challenges, we introduce hypercurves, a flexible framework for answering approximate k-nearest neighbor (kNN) queries for very large multimedia databases, aiming

at online content-based multimedia services. Hypercurves executes on hybrid CPU–GPU environments, and is able to employ those devices cooperatively to support massive query request rates. In order to keep the response times optimal as the request rates vary, it employs a novel dynamic scheduler to partition the work between CPU and GPU. Hypercurves was thoroughly evaluated using a large database of multimedia descriptors. Its cooperative CPU–GPU execution achieved performance improvements of up to 30× when compared to the single CPU-core version. The dynamic work partition mechanism reduces the observed query response times in about 50% when compared to the best static CPU–GPU task partition configuration. In addition, Hypercurves achieves *superlinear* scalability in distributed (multi-node) executions, while keeping a high guarantee of equivalence with its sequential version — thanks to the proof of probabilistic equivalence, which supported its aggressive parallelization design.

E. Valle and R. Torres thank FAPESP for the financial support to this work. Preprint — submitted for peer review.

G. Teodoro(✉) and J.H. Saltz
Center for Comprehensive Informatics, Emory University, GA, USA
E-mail: {gteodor,jhsaltz}@emory.edu

E. Valle
Recod Lab / DCA / FEEC, State University of Campinas, SP, Brazil
E-mail: dovalle@dca.fee.unicamp.br

N. Mariano and W. Meira Jr
Department of Computer Science, Universidade Federal de Minas Gerais, MG, Brazil
E-mail: {nathanr,meira}@dcc.ufmg.br

R. Torres
Recod Lab / DSI / IC, State University of Campinas, SP, Brazil
E-mail: rtorres@ic.unicamp.br

Keywords Descriptor indexing · Multimedia databases · Information retrieval · Hypercurves · Filter-stream · GPU

1 Introduction

Similarity search is the process of finding among objects stored in a reference database, those nearest to a query object. In multimedia processing, both the query and the database objects are represented by a feature vector in a high-dimensional space. Several choices are available to establish the notion of distance,

Euclidean distance being the most common. That operation is of fundamental importance for several applications in content-based multimedia retrieval services, which include not only search engines for web images [42] but also image recognition on mobile devices [27], real-time song identification [10], photo tagging in social networks [50], recognition of copyrighted material [58] and many others. Nowadays, those services instigate an exciting scientific frontier and impel a multimillionaire consumer market.

Though those services may appear extremely diverse, they are all founded upon the use of descriptors, which extract feature vectors from multimedia documents, thus giving them a perceptually meaningful geometry. The descriptors allow us to bridge the so called “semantic gap”: the disparity between the amorphous low-level coding of multimedia, e.g., image pixels or audio samples, and the complex high-level tasks, e.g. classification or document retrieval, we need to perform. Looking for similar documents becomes equivalent to looking for similar vectors. The actual query processing may be complex, consisting of several phases, but similarity search will often be the first step and, because of the (in-)famous “curse of dimensionality”, one of the most expensive.

The success of current content-based multimedia retrieval services depends on their ability to handle extremely large and increasing volumes of data, and keep the response times observed by the end-user low. The databases needed to process even a tiny fraction of the images available in the Web are larger than the storage capacity of most commodity single-user machines. The great majority of indexing methods for similarity search, however, were designed to execute sequentially, and are not able to take advantage of the aggregate power in distributed environments. Moreover, classical distributed algorithms tend to ignore the response-time of processing each individual query, and to concentrate in providing maximum throughput for batches of queries. That strategy clashes with the online nature of content-based multimedia retrieval services, because just like on other search engines, the waiting time observed by individual user requests is critical. Moreover, online interaction between user and services creates large variations in the query rates submitted to the system, requiring those systems to adapt continuously to better exploit the available hardware and lower the response times whenever possible.

In order to address these challenges, in this work, we propose Hypercurves, a concurrent index built upon the sequential multidimensional index Multicurves [59,60] and the concurrent execution environment Anthill [51,53]. Multicurves addresses the challenges of approximate similarity queries for multimedia services, including an optimizing scheduler that adapts the parallelization regimen online to minimize query response-times under fluctuating request loads. Hypercurves near-linear speedups and super-linear scaleup on distributed environments rest upon the fact that Multicurves design fits extremely well into the filter-stream execution model implemented in Anthill. Nevertheless, the transition from sequential to parallel indexing remains very challenging, and depends crucially on the ability of accessing independently each partition of the data. We demonstrate that this can be done efficiently, while keeping the algorithms equivalent with very high probability (Section 4.2).

Hypercurves was published in preliminary form in [56], where we evaluated its performance in CPU-only multi-core distributed machines. Though it performed extremely well as compared to the sequential version, its performance remained constrained by the compute-intensive task of evaluating distances between the query feature vector and hundreds of candidate vectors. In this paper, we address that shortcoming by redesigning Hypercurves for execution on heterogeneous environments, comprising both CPUs and GPUs (graphical processing units). GPUs are massively parallel and power-efficient processors, which have found a niche as accelerators for regular compute-intensive applications. The utilization of GPUs with Hypercurves, however, is very challenging, since we are interested in providing low response times under online workloads that vary throughout execution. GPUs, on the other hand, are fundamentally throughput-oriented, because they are built as a large collection of low-frequency computing cores, which are able to process a very large number of simple operations in parallel.

In Hypercurves, therefore, queries dispatched for execution with a GPU may observe higher average response times, as they are using a collection of less powerful GPU computing cores as compared to a CPU core. Thus, a carefully scheduling is employed to decide the best partition of queries between CPUs and GPUs in order to minimize the average query

response times during the execution. This problem is specially critical in Hypercurves as the best partition is affected by the load of requests submitted to the system throughout the execution.

In this paper, we address these challenges, obtaining a dramatic improvement on top of the former version of Hypercurves [56]. The techniques we use to schedule tasks for Hypercurves are also generalizable to other online applications that benefit from GPU accelerations. The key contributions include:

1. An improved Hypercurves, able to employ GPUs concurrently to answer a massive number of requests in very large databases;
2. A careful design and implementation of optimizations for the parallelization in hybrid CPU–GPU environments, including cooperation CPU–GPU execution and asynchronous execution between these devices, as detailed in Section 5. This version achieved speedups of about $30\times$ as compared to the CPU-only single core version of the application;
3. A dynamic scheduler algorithm for hybrid CPU–GPU environments, which employs both devices cooperatively in order to minimize response times, and is able to adapt the application automatically under fluctuating request loads to optimize response times. When compare to the best static partition, the scheduler obtained average query response times up to 48% smaller.

All contributions are thoroughly evaluated in a comprehensive set of experiments.

The remainder of the text is organized as follows. In the next section, we discuss content-based multimedia services, examining how the problem of similarity search is critical to their success. Section 3 summarizes the algorithmic foundations of this work, by presenting the sequential index Multicurves, and the parallel framework Anthill, which is used to build our parallel index Hypercurves. Hypercurves parallelization strategy is detailed in Section 4 along with an analytical proof of the probabilistic equivalence between Multi- and Hypercurves. Section 5 introduces progressively sophisticated execution plans for Hypercurves on heterogeneous CPU–GPU environments. Section 6 discusses scheduling considering heterogeneous CPU–GPU environments, under online time constrained applications as Hypercurves. In Section 7 we present an experimental evaluation of the proposed scheme in many stress

scenarios, proceeding to the conclusions in Section 8.

2 Related work

In textual data, low-level representation is strongly coupled with semantic meaning because the correlation between textual words and high-level concepts is strong.

In multimedia, by contrast, the low-level coding (pixels, samples, frames) is extremely distant from the high-level semantic concepts needed to answer the user queries, precipitating the much debated “semantic gap”. In order to overcome that difficulty, it is necessary to embed the multimedia documents in a space where distances represent perceptual dissimilarities: that is the task of **descriptors**. The descriptors are an essential first step towards bridging the gap between the amorphous low-level coding and the high-level semantic concepts.

Multimedia descriptors are very diverse, including a large choice of representations for perceptual properties that may help to understand the documents. Those properties include shape, color and texture for visual documents; tone, pitch and timbre for audio documents; flow and rhythm of movement for moving pictures; and many others. The descriptor gives these perceptual properties a precise representation, by encoding them into a **feature vector**. That induces a geometric organization where perceptually similar documents are given vectors near in the space, while perceptually distinct documents are given vectors further apart. To establish those distances, often a simple metric is employed, like the Euclidean or the Manhattan, but sometimes more complex metrics are chosen [42].

Especially in what concerns images and videos, the last decade witnessed the ascent of descriptors inspired by Computer Vision, especially the so-called *local descriptors* [38,57], with the remarkable success of SIFT [33]. As their name suggests, local descriptors represent the properties of small areas of the images or videos (in opposition to the traditional *global descriptors*, which attempt to represent the entire document in a single feature vector). Their success was followed by the idea of using compact representations based on their quantization using codebooks, in the so-called “bag of visual words” model, which became one of the main tools in the literature [7].

Regardless of the specific choice, the retrieval of similar feature vectors becomes a cornerstone operation to almost all systems. That operation can be used either directly (many early CBIR systems were little more than a similarity search engine attached to a descriptor space [49]), either indirectly (similarity search may be part of a kNN classifier, it can retrieve a preliminary set of candidates to be refined by a more computationally intensive classifier, etc.). In one way or another, it remains a critical component, if the system is to be used in real-world, large-scale databases [32].

We can formalize the problem of search with multimedia descriptors in the framework of feature-based processing of similarity queries of Böhm et al. [6]. The multimedia description algorithm corresponds to the feature vector extraction, which, formally is a function F that maps a space of multimedia objects Obj into d -dimensional real vectors:

$$F : Obj \rightarrow \mathbb{R}^d \quad (1)$$

Now, the dissimilarity between two objects $obj_i \in Obj$ can be determined by establishing the distance (e.g., Euclidean) between their feature vectors:

$$\Delta(obj_1, obj_2) = \|F(obj_1), F(obj_2)\| \quad (2)$$

Given that dissimilarity between objects, we can establish several types of similarity queries [6] (range, nearest neighbor, k nearest neighbors, inverse k nearest neighbors, etc.). In this work, we are especially interested in k nearest neighbors queries (kNN, for short). Given a database $B \subseteq Obj$ and a query $q \in Obj$, the k nearest neighbors to q in B are the indexed set of the k objects in B closest to q :

$$\text{kNN}(B, q, k) = \{b_1, \dots, b_k \in B \mid \forall i \leq k \\ \forall b \in B \setminus \{b_1, \dots, b_i\}, \Delta(q, b_i) \leq \Delta(q, b)\} \quad (3)$$

That defines the *exact* version of kNN search. As we will see, for large-scale multimedia services, that definition will have to be relaxed to account for approximate answers, which allows for dramatic gains in speed.

2.1 Prior Art

Efficient query processing for multidimensional data has been pursued for at least four decades,

with a myriad of applications that go far beyond multimedia feature vector matching. Those include satisfying multi-criteria searches, and searches with spatial and spatiotemporal constraints [16, 19, 41, 62].

An exhaustive review would be overwhelming and beyond the scope of this article. The most comprehensive reference to the subject is the textbook of Samet [45]. The book chapters of Castelli [9] and Faloutsos [21] provide a less daunting introduction, more focused on content-based based retrieval for images. Another comprehensive, if somewhat old, reference is the survey of Böhm et al. [6], which also provides an excellent introduction to the theme, with a good formalization of similarity queries, the principles involved in their indexing and their cost models. The book edited by Shakhnarovich et al. [47] focuses on computer vision and machine applications. In what concerns metric methods, which are able to process non-vector features, as long as they are embedded in a metric space, the essential reference is the textbook of Zezula et al. [64]. Although already decade-old, the survey of Chávez et al. [11] is also an excellent, comprehensive introduction to similarity search in metric spaces.

Despite the huge assortment of methods available, those of practical interest in the context of large-scale content-based multimedia services are surprisingly few. Because of the “curse of dimensionality” (explained below), methods that insist on exact solutions are only adequate for low-dimensional spaces, while multimedia feature vectors often have hundreds of dimensions. Most methods assume that the implementation uses shared main memory (with cheap uniform random access), which cannot be the case on the very large databases we want to address. Other methods, such as the ones based on clustering, have prohibitively high index building times (with a forced rebuilding if the index changes too much), being adequate only for moderate-size static databases.

The focus of multimedia retrieval and classification on approximate techniques is not just a result of the technical challenge of treating high dimensionalities. Multimedia descriptors are always intrinsically approximate, due to the fact the relationship between the visual properties they encode and the high-level semantic concepts remains limited. In addition, descriptors almost always employ quantization and averaging to various degrees, making them approx-

imate also in a numerical and statistical sense. Therefore, insisting on exact techniques makes no sense. What is needed is a good trade-off between precision and speed.

Approximation in kNN search may imply different compromises: sometimes it means finding elements not too far from the exact answers, i.e., guaranteeing that the distance to the elements returned will be up to a factor from the distance to the correct elements; sometimes it means a bounded probability of missing the correct elements. Sometimes, the guarantee offered is more complex than that, for example, a bounded probability of finding the correct answer, provided it is sufficiently closer to the query than the closest incorrect answer [28].

Approximation on a bounded factor is formalized as following: given a database $B \subseteq Obj$ and a query $q \in Obj$, the $(1+\epsilon)$ k nearest neighbors to q in B are an indexed set of objects in B whose distance to the true kNN is at most a $(1 + \epsilon)$ factor higher:

$$\epsilon\text{-kNN}(B, q, k) = \left\{ b_1, \dots, b_k \in B \mid \begin{array}{l} \forall i \leq k, [\forall b \in B \setminus \{b_1, \dots, b_i\}, \\ \Delta(q, b_i) \leq (1 + \epsilon) \Delta(q, b)] \end{array} \right\} \quad (4)$$

Some methods might only guarantee such results with a probability bounded by some constant. More often than not, however, practical approximative methods offer no formal guarantees, but just good empirical performance.

If perfect accuracy can be excused, the efficiency requirements remain very challenging: the method should perform well for high-dimensional data (hundreds of dimensions) in very large databases (at least millions of records); it must adapt well to secondary-memory storage, which in practice means that few random accesses should be performed; it should be dynamic, i.e., allow data insertion and deletion without performance degradation.

A common pattern found in methods useful for large-scale multimedia is a strategy of projecting the data onto different subspaces and creating **subindexes** for each of those subspaces. The subindexes can be queried more or less independently, and the results aggregated to find the final answer.

MEDRANK is one of those methods, which projects the data into several random straight lines. The one-dimensional position in the line is used to index the data [18]. The method

has an interesting theoretical analysis, establishing that under certain hypotheses, rank aggregation on straight line projections offers some (lax) bounds on approximation error. The techniques employed by the algorithm were extremely well succeeded in moderately-dimensional multi-criteria databases, for which it is still feasible to search for exact solutions. In those cases, many of the choices are provably optimal [19]. For high-dimensional multimedia information, however, the technique fails, mainly due to the lack of correlation between the distance in the straight lines and the distance in the high-dimensional space [58].

Locality-sensitive hashing (LSH) uses locality-aware hashing functions to index the data. The method uses several of those “hash tables” at once, to improve reliability [28]. LSH is backed by an interesting theoretical background, which allows predicting the approximation bounds for the index, for a given set of parameters. The well-succeeded family of pStable locality sensitive hash functions [13] has allowed LSH to directly index Euclidean spaces, and its geometric fundament is also strongly based on the idea of projection onto random straight lines. LSH works extremely well when one wants to minimize the number of distances to be evaluated, and can count on uniform cost random access to the data. However, in situations where the cost of accessing the data dominates the cost of computation, its efficiency is compromised. The parameterization of LSH tends to favor the use of a large number of hash functions (and thus subindexes), which also poses a challenge for scalability.

An interesting family of solutions employs the fractal space-filling curves. Like MEDRANK, those methods reduce multidimensional indexing to one-dimensional indexing, but using more sophisticated projections. The method upon which we build our work, Multicurves, is one of those methods and it is explained in more detail on Section 3.1. Since that family of methods is particularly related to our work, we focus our review on them.

2.2 Indexing with Space-filling Curves

Space-filling curves are maps from the unit interval to a hypercube of any dimensionality [44]. Most of those curves are constructed by fractal, self-similar, recursive procedures. Although the curves are fascinating in themselves,

here we are interested in their ability to induce a “vicinity-sensitive” total order in the data. With good probability, they preserve neighborhood relations: if point A is closer to point B than to point C in the space, that relationship tends to remain in the curve (Figure 1).

Space-filling curves have been implicitly used to perform similarity searches in multidimensional spaces for a very long time. Indeed, one of the first multidimensional indexes ever proposed [39] employed them hidden in the idea of “bit shuffling”, “bit interlacing” or “bit interleaving”, which consisted in interleaving the bits of the individual space coordinates to generate a search key. Interleaving the bits, in fact, induces a type of space-filling curve called Z-order curve, which explains why the method works well. However, it was Faloutsos [20] the first to explicitly refer to the concept of curves, and were Faloutsos and Roseman [22] the first to suggest the use of curves other than the Z-order, first proposing the Gray-code curve and then the Hilbert curve.

Those pioneering methods worked in a very simple way, using the curve to map the multidimensional vector onto a one-dimensional key representing the position in the curve (which we call here *extended-key*). That position was then employed to perform the search by similarity. For example, when performing kNN search, a good heuristic is to take the nearest elements in the curve as the nearest elements in the space, because of the “vicinity-sensitiveness” explained above.

Unfortunately, points near in the space are not always near in the curve. In fact, the biggest problem when employing the curves is the existence of boundary regions where the neighborhood-relation preserving properties are violated, and points closer in space are placed further apart in the curve (Figure 1). That issue worsens dramatically as dimensionality grows [30, 48].

In order to conquer the boundary effects, Megiddo and Shaft [37] suggested the use of several curves at once. As is done for the multiple straight lines of MEDRANK, or for the multiple hash-tables of LSH, we build an independent subindex for each curve. The query is then sought on all subindexes, in the hope that in at least one of them, it will not fall close to a boundary region. Megiddo and Shaft present the idea in very general terms, without describing which types of space-filling curves should be used and what had to be done to

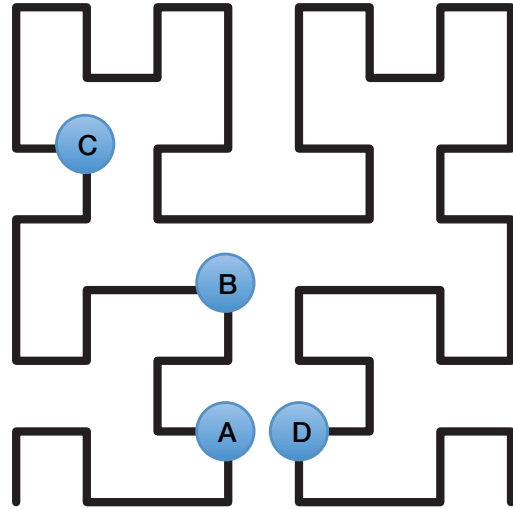


Fig. 1 Space-filling curves provide a “vicinity-sensitive” map: relative closeness in the space tends to be preserved in the curve (points A, B and C). However, in some boundary regions, those properties are violated (points A, B and D).

make them different. Therefore, Shepherd et al. [48] developed that idea, specifically recommending the use of several identical Hilbert curves, where different copies of the vectors are transformed by random rotations and translations. Whether or not those transformations could be optimized was left unanswered. Finally, Liao et al. [30] solved the problem of choosing the transformations, by devising the necessary number of curves and an optimal set of translations to obtain (lax) bounds on the approximation error in the case of kNN search.

A depart from those methods was suggested by Mainar-Ruiz and Pérez-Cortés [35]. Instead of using multiple curves, they propose using multiple instances of the same element in only one curve. Before inserting those instances in the curve, the algorithm disturbs randomly their position, to give them the opportunity of falling into different regions of the curve. In that way even if the query falls in a problematic region, chances are it will be reasonably near to at least one of the instances. Akune et al. improved on that method, by proposing a more careful placement of the instance copies on the curve [1], obtaining thus a significant improvement in precision.

Another depart was suggested by Valle et al. in Multicurves [59, 60], which also employed several curves, but with the important difference that each curve maps a projection of

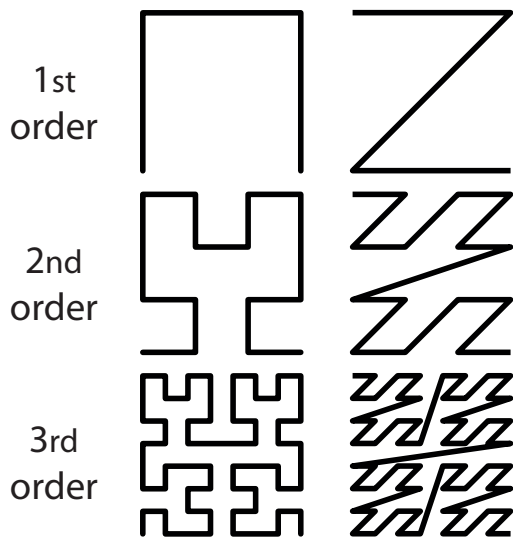


Fig. 2 Space-filling curves are usually obtained by a recursive refinement procedure, resulting in a fractal, self-similar curve. Each refinement step is called a *order* of the curve. The curve fills the Continuum at the infinite limit of that procedure, but for working on digital data, it is not necessary to reach that limit. The figure shows three successive steps of the Hilbert curve (left) and the Z-order curve (right).

the vectors onto a moderate-dimensional subspace. That dimensionality reduction makes for an efficient implementation, reducing the effects of the “curse of dimensionality”. Because of the exponential nature of the “curse” it is more efficient to process several low or moderate-dimensional indexes than a single high-dimensional one. That is explained by the fact that we do not only gain the intrinsic advantages of using multiple curves (i.e., elements that are incorrectly separated in one curve will probably stay together in another), but also, we lower the boundary effects inside each one of the curves. Multicurves is explained in detail in Section 3.1.

2.2.1 Technical Details

Space-filling curves are fractal curves introduced by G. Peano and D. Hilbert [44], which provide a continuous surjective map $C : [0, 1] \rightarrow [0, 1]^d$ from the unit interval to a hypercube of any dimensionality. Most of those curves are constructed by recursive procedures, where, in the limit, the curve fills the entire space (Figure 2).

It was already known (due to a result of E. Netto) that such a mapping C could not be at once bijective and continuous. Dropping in-

jectivity, Peano was able to construct the first known continuous surjective map from the line to the space. Interestingly, in the recursive procedure to build the curve, all finite steps are bijective, but the limiting (and thus, effectively space-filling) curve becomes self-intersecting. In our applications with digital data, we can always consider C bijective, because we never reach the limit needed to deal with the true Continuum.

When using the space-filling curve map in indexing, we are interested in the pre-images of the query and data points. Using the same notation as before, for $b_i \in B$ and $q \in Obj$, we are interested in those $C^{-1}(F(b_i))$ which are close to $C^{-1}(F(q))$ (remember that F is the function that maps multimedia objects into feature vectors). We call the pre-image $C^{-1}(x)$ the **extended-key** of feature vector x .

There is a direct relationship between the number of refinements we need to go through in the recursive curve (called the *order* of the curve) and the precision of the data we want to index. If we are employing dyadic curves (like the Z-order, Gray-order or Hilbert curves), we need m^{th} order curves to index coordinates of m bits. Remark that the bijective map C^{-1} preserves the number of bits: from d coordinates of m bits each to a single extended-key with $d \times m$ bits.

It is important to emphasize that the curve does not have a concrete representation in the indexes. That is a common source of confusion for those who get acquainted for the first time with indexing based on space-filling curves. The curve is an useful abstraction, employed to create the map C^{-1} , which generates “neighborhood-sensitive” extended-keys. Then, the extended-keys are used in conventional, one-dimensional, indexing structures (a hash-table, a B-tree, etc.).

The actual computation of C^{-1} depends, of course, on the type of space-filling curve being employed. For the Hilbert curve, several recursive algorithms have been proposed, but the most efficient scheme is an iterative one [8]. As we have mentioned, for the Z-order curve, the computation is extremely simple: it suffices to intercalate the bits of the coordinates.

It is interesting to analyze which kind of data can be indexed by the curves. The curves are able to organize vectors of any fixed-length ordinal data, provided that the order is the “natural” one: the order of the data is the same order of the numbers (binary codes) in which

they are encoded. Otherwise, a transformation must be used to translate the vector of data into a vector of orders.

In the case of multimedia descriptors, we are mainly interested in vectors of numeric data. When the coordinates are integer, it is easy to see the scheme works, although the programmer must ensure to deal correctly with negative numbers in C^{-1} . Although less obvious to see, the scheme works with almost no modification for (IEEE 754) floating-point numbers. Indeed, because in that encoding the bits of the exponent are in more significant positions than the bits of the mantissa, the order of the encoded numbers is “natural”. Again, the only caveat is to deal correctly with the most significant sign bit, used for negative numbers.

3 Background

This section presents an introduction to Multicurves, the algorithmic foundation, upon which our parallel solution is built; and details Ant-hill, the dataflow-based framework employed in the parallelization.

3.1 The Sequential Index Multicurves

Multicurves [59,60] is an index for accelerating kNN queries based on space-filling curves. Its properties make it especially adapted for large-scale multimedia databases.

As we have seen in Section 2.2, the greatest problem in using space-filling curves comes from boundary effects brought by the existence of regions where their neighborhood-relation preserving properties are violated. Different methods propose different solutions, usually through the simultaneous use of multiple curves. As we have mentioned, Multicurves is also based on the use of multiple curves, but with the important improvement that each curve is only responsible for a subset of the dimensions. Because of the exponential nature of the “curse”, it is more efficient to process several low-dimensional queries than a single high-dimensional one.

Multicurves index construction is simple (Algorithm 1). The feature vector for each database element is obtained (almost always, it will be computed beforehand, so the operation in line 3 just retrieves the corresponding field). The dimensions of the feature vectors are divided among a certain number of subindexes

Algorithm 1 Multicurves index construction

input:

B : the database elements to be indexed
 $curves$: number of curves (and, thus, of subindexes)
 $dims[i]$: dimensionality of the i^{th} curve
 a : attribution of the feature vectors dimensions to the subindexes — $a[i, j]$ is the dimension in the i^{th} subindex to which the j^{th} dimension of the input data should be attributed (see line 7 below)
 $C^{-1}()$: the space-filling curve map, as explained in Section 2.2.1
 $F()$: the description function, returning a feature vector, as explained in Section 2. Usually, that will be already precomputed.

output: an array of $curves$ sorted lists, which composes the index (each element is a subindex)

```

1:  $subindexes[] \leftarrow$  new array with  $curves$  empty sorted lists;
2: for all  $b \in B$  do
3:    $v \leftarrow F(b)$ ;
4:   for  $c \leftarrow 1$  to  $curves$  do
5:      $proj[] \leftarrow$  new array with  $dims[c]$  empty elements;
6:     for  $d \leftarrow 1$  to  $dims[c]$  do
7:        $proj[d] \leftarrow v[a[c, d]]$ ;
8:        $key \leftarrow C^{-1}(proj)$ ;
9:       Insert  $\langle key, b \rangle$  into  $subindexes[curve]$ ;
10: return  $subindexes[]$ ;
```

based on a space-filling curve. Geometrically, that can be understood as projecting the feature vector onto a subspace and then mapping it using a curve that fills the subspace. For didactical reasons, the algorithm is presented as a “batch” operation, but nothing prevents the index from being built incrementally, as long as the structure used to back the sorted lists allows so.

The search is conceptually similar: the query is decomposed into projections (whose subspaces must be the same used during the index construction) and each projection has its extended-key computed. Then, from each subindex, we obtain a certain number of candidate elements (**probe-depth**), whose extended-keys are the nearest to the extended-key of the corresponding projection of the query. In the end, we compute the actual distance from those elements to the query and keep the k nearest (Algorithm 2).

The index creation and search processes are illustrated in Figure 3.

It should be noted that in the scheme shown above, for simplicity sake, we supposed that both the query and the database elements are associated with a single feature vector by the

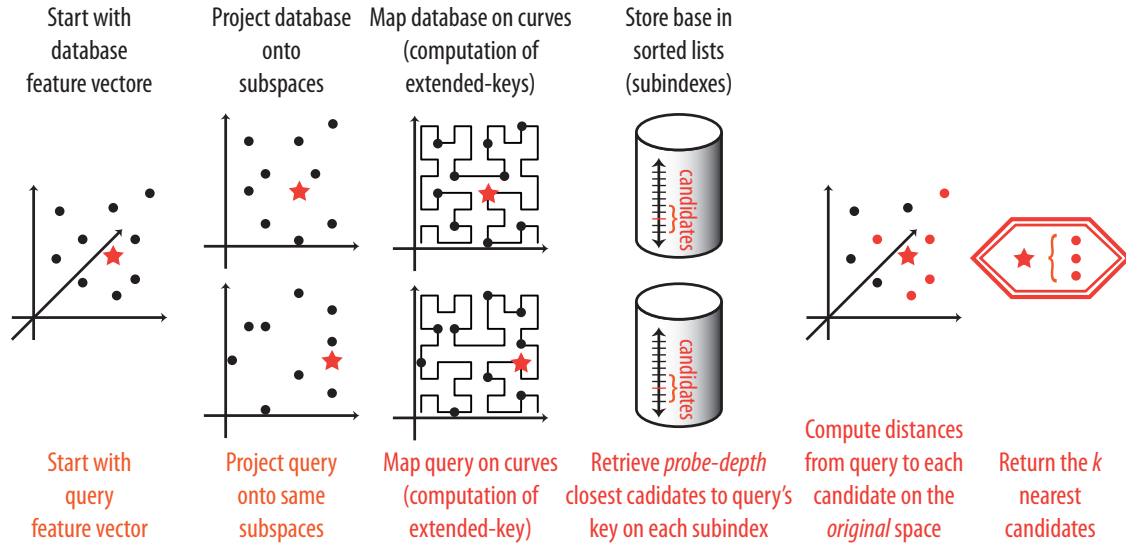


Fig. 3 Multicurves in action. (In black:) The index is created by projecting the database feature vectors (small dots) onto different subspaces and mapping each projection in a space-filling curve to obtain the extended-keys. Each subspace induces an independent subindex, where the vectors are stored, sorted by extended-keys. (In red:) Searching is performed by projecting the query feature vector (red star) onto the same subspaces and computing the extended-keys of the projections. A number (probe-depth) of candidates closest to the query's extended-key is retrieved from each subindex. Finally, the true distance of the candidates to the query is evaluated and the k closest are returned.

Algorithm 2 Multicurves search phase

input : (in addition to $curves$, $dims[]$, $a[]$, $C^{-1}()$ and $F()$ explained in Algorithm 1)

k : the number of desired nearest neighbors

$depth$: the probe-depth, i.e., the number of elements to examine per subindex

q : the data element to be queried

$subindexes[]$: array of sorted lists composing the index, generated in Algorithm 1)

output : a list with the k approximate nearest neighbors

```

1:  $v \leftarrow F(q)$ ;
2:  $candidates \leftarrow \emptyset$ ;
3: for  $c \leftarrow 1$  to  $curves$  do
4:    $proj[] \leftarrow$  new array with  $dims[c]$  empty elements;
5:   for  $d \leftarrow 1$  to  $dims[c]$  do
6:      $proj[d] \leftarrow v[a[c, d]]$ ;
7:    $key \leftarrow C^{-1}(proj)$ ;
8:    $candidates \leftarrow candidates \cup \{depth \text{ closest vectors to } key \text{ in } subindex[c]\}$ ;
9:  $knn \leftarrow \{k \text{ closest vectors to } q \text{ in } candidates\}$ ;
10: return  $knn$  ;
```

description function $F()$. The extension of the algorithm is trivial for descriptors (like local descriptors) that generate several vectors per multimedia object, but bear in mind that the each vector is indexed and queried independently (for example, if a query object generates 10 feature vectors, the kNN search will produce 10 sets of k nearest neighbors, one for

each query vector). The task of taking a final decision (classification result, retrieval ranking) from those multiple answers is very application-dependent and beyond the scope of our article, which is concerned with the basic infrastructure. Here, we are concerned in achieving efficiently good results for each individual query vector.

In an experimental evaluation [59,60] on high-dimensional feature vectors, Multicurves compared favorably to the state of the art, represented by the methods of Liao et al. [30] and Mainar-Ruiz and Pérez-Cortes [35], presenting a better compromise between precision and speed. It also performed well [60], when compared to LSH [13], presenting an equivalent compromise between precision and number of distances computed, but performing fewer random accesses.

3.2 The Parallel Environment Anthill

Anthill [53,51,55,52,23] is a run-time system based on the filter-stream programming model [3] and, as such, applications are decomposed into processing stages, called *filters*, which communicate with each other using unidirectional *streams*. At run time, Anthill spawns, on the nodes of the cluster, instances of

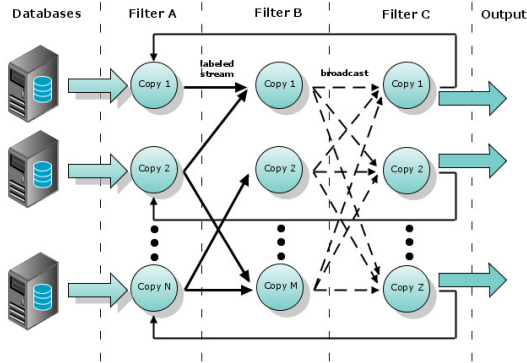


Fig. 4 The architecture of an Anthill application. Filters (columns) cooperate to process the data. Their communication is mediated by unidirectional streams (arrows). The filters are instantiated in transparent copies (circles) automatically by Anthill’s runtime. The non-blocking I/O flow and event scheduling is also handled by Anthill.

each filter, which are called transparent copies, and automatically handles communication and state partitioning among those copies [51].

When developing an application using the filter-stream model, both task and data parallelism are exploited. Task parallelism is achieved as the application is broken up into a set of filters, which perform independently, accomplishing the application functionality in a pipeline fashion. Data parallelism, on the other hand, is obtained by creating transparently multiple copies of each filter and distributing the data to be processed among them (Figure 4).

Anthill provides an event-oriented filter programming abstraction, deriving heavily from the message-oriented programming model [4, 40, 61]. The streams that establish the communication between filters generate input events, which must be handled. The programmer provides handling functions for those events. Anthill runtime instantiates those functions and controls the non-blocking I/O flow to keep the system running. It is a dataflow model, where event handling amounts to asynchronous and independent tasks. Because the filters are multithreaded, multiple tasks can be spawned when there are enough pending events and computational resources. That feature is essential both in exploiting the full capability of current multi-core architectures, and in spawning tasks on multiple devices in heterogeneous, CPU-GPU equipped platforms. That flexibil-

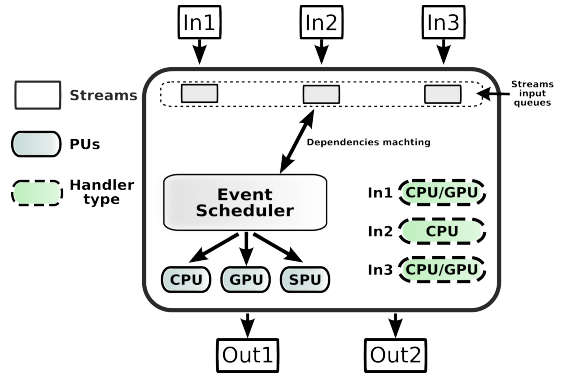


Fig. 5 The architecture of a single filter. Input streams (top blocks) generate events that must be handled by the filter. Different handler functions (dashed round boxes) can be provided by the programmer for each type of event and processing unit. The event scheduler coordinates the filter operation, dequeuing the input events and invoking the handling functions according to the available processing units (round boxes). As processing progresses, data is sent to the output streams (bottom blocks), generating events on the next filter (not shown).

ity is accomplished by allowing the programmer to provide, for the same event, handler functions targeting different devices which can be invoked by the scheduler to use the appropriate processor.

Figure 5 illustrates the architecture of a typical filter (a single application will be composed of several of those). It receives data from multiple input streams (*In1*, *In2*, and *In3*), each generating its own event queue, with handler functions associated to each of them. As shown, those functions are implemented targeting different types of processors. The *Event Scheduler*, depicted in the picture is responsible for consuming events from the queues, invoking appropriate handlers according to the availability of computational resources. As events are consumed, eventually some data is generated on the filter that will be forwarded to the next filter. As those data arrive in the next filter, they will trigger input events there. All filters run in parallel. Communication between filters, although not shown in the figure, is also managed by the run-time system.

When events are queued, they are not immediately assigned to a processor. Rather, that occurs on-demand, as devices become idle and request new events to process. In the current implementation, the demand-driven, first-come, first-served (DDFCFS) task assignment policy is used as default strategy of the Event Scheduler.

The first decision for the DDFCFS policy is to select from which queue to execute events; this decision is made in a round-robin fashion, provided the event has a handling function compatible with the available processor. The oldest event on the selected queue is dispatched for processing. That simple approach guarantees assignment to different devices according to their relative performance in a transparent way, as processors will consume events in proportion to their capacity to process them.

4 The Distributed Index Hypercurves

In this section, we discuss how Multicurves (Section 3.1) has been redesigned for efficient execution on distributed environments, focusing on the CPU-only version of the application (details of the GPU-based presented in Section 5).

Further, we present a proof of the probabilistic equivalence between Multicurves and Hypercurves (Section 4.2). The proof is essential for the efficiency of the scheme, because in Hypercurves, the database is partitioned without overlapping among the nodes in the execution environment. Search is performed locally in the subindexes managed by each node, and a reduction stage merges the results. The cost of the algorithm is dominated by the local searches, which are further dependent on the probe-depth used (the number of candidates to retrieve from each subindex). When using the same probe-depth of the sequential algorithm for each local index of the distributed environment, the answer of Hypercurves is guaranteed at least as good as the sequential algorithm. However, that is an extremely pessimistic and costly choice for the local indexes probe-depth: we show that the quality of Hypercurves is equivalent to that of Multicurves with very high probability, when using a probe-depth slightly higher than the original probe-depth divided by the number of nodes.

The ability to avoid data replication improves the scalability of the solution. The user can further modify the probe-depth of the parallel algorithm according to Equation 5 (Section 4.2), to guarantee that the quality of Hypercurves is equivalent to that of Multicurves with any desired probability.

4.1 Hypercurves Parallelization Strategy

Hypercurves [56] is a concurrent index built upon the sequential multidimensional index Multicurves [60] and the concurrent execution environment Anthill [51], in order to provide approximate similarity search support for large-scale online multimedia services. Therefore, Hypercurves addresses both the need to scale the database to sizes beyond the capability of a single machine, and the need to keep the answer times as short as possible.

Hypercurves strategy is to partition the database among the nodes (*filter copies* in the nomenclature of Anthill) of the distributed environment. The queries are broadcast to all filter copies, which find a local answer in their database subsets. The local answers are then reduced to a global answer in a later merge step.

To better exploit Anthill execution environment, Hypercurves employs four types of filter, organized in two parallel computation pipelines (Figure 6).

The first pipeline is conceptually an index builder/updater, with the filters *Input Reader* (IRR) and *Index Holder/Local Searcher* (IHLS). IRR reads the feature vectors from the input database and partitions them among the copies of IHLS, which add the vectors received to their local index, according to Algorithm 1. The filters execute concurrently, and after the input is exhausted, interact to update the database.

The second pipeline, which is conceptually the query processor, contains three filters: (i) *Query Receiver* (QR); (ii) IHLS (shared with the first pipeline); and (iii) *Aggregator*. QR is the entry point to the search server, receiving and broadcasting the queries to all IHLS copies. For each query, IHLS instances independently perform the search on their local index partition, retrieving k nearest *local* feature vectors just like the sequential Multicurves (Algorithm 2). The final answer is obtained by the Aggregator filter, which reduces the local answers into k *global* nearest vectors. Since several Aggregator filter copies may exist, it is crucial that the messages related to a particular query (same query-id) be sent to the same Aggregator instance. That is guaranteed by making full use of Anthill Labeled-Stream communication policy, which computes the particular copy of the Aggregator filters that will receive a given message sent from IHLS based on a *hash* com-

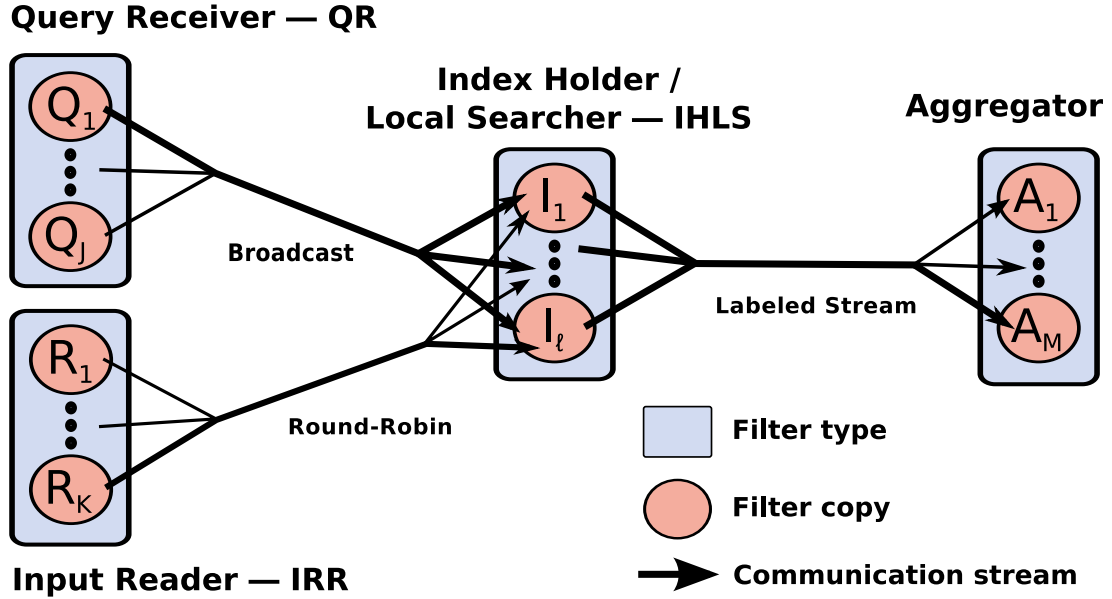


Fig. 6 Hypercurves parallelization design. Four filter types are involved: IRR, which reads data from the database and dispatches them to the IHLS to be indexed; QR, which reads queries from the user and dispatches them to the IHLS to be processed; IHLS, which provides a “local” index and query processing, for a subset of the data; Aggregator, which collects local kNN answers to the queries and aggregates them into a global kNN answer. Transparent copies of those filters are instantiated as needed by Anthill’s runtime. Several types of streams are used in the communication between those copies: for example, during search, a query is broadcast from QR to all copies of IHLS; then all local answers relative to that query are sent to the same Aggregator filter, using the “labeled stream” facility.

puted in the query-id. Therefore, in this context, query-id corresponds to the label of the message. The transaction between IHLS and Aggregator is very similar to a generalized parallel data reduction [63], except that it outputs a list of values for each output, and that an arbitrary number of reductions are executed in parallel.

Hypercurves exploits all four dimensions of parallelism: task, data, pipeline, and intra-filter. Task parallelism occurs as the two pipelines are executed in parallel (e.g., index updates and searches). Data parallelism is achieved as the database is partitioned among the IHLS filters copies. Pipeline parallelism results from Anthill ability to execute in parallel the filters of a single computational pipeline (e.g., IRR and IHLS for updating the index). Intra-filter parallelism refers to a single filter copy being able to process events in parallel, thus, efficiently exploiting modern multi- and many-core computers.

The broadcast from QR to IHLS has little impact on performance, because the cost is dominated by the local searches. Therefore, the communication latency is offset by the computation speedups. The disproportionate cost of

those searches has prompted a GPU-based implementation (Section 5), which in turn raised interesting challenges to the scheduling of the pipelined events, leading to another important contribution of this work (Sections 6).

The cost of local searches depends critically on the probe-depth used (the number of candidates to retrieve from each subindex). Hypercurves can be made assuredly equivalent to Multicurves, by employing on each parallel node a probe-depth at least as large as the one used in the sequential algorithm. However, this over-pessimistic choice is unnecessarily costly and can be significantly improved, as we will see in the next section.

4.2 Probabilistic Equivalence Multicurves–Hypercurves

Multicurves is based upon the ability of space-filling curves giving a total order to data. That makes each subindex a sorted list where a number of candidates can be retrieved and then verified against the query in order to obtain the k nearest (Algorithm 2).

In Hypercurves, the index is fragmented, with each IHLS filter copy having available only a subset of the database: a single filter cannot warrant the equivalent approximate k nearest neighbors. That is the role of the Aggregator filter: collecting the local best answers and returning a final solution.

In terms of equivalence between Multi- and Hypercurves it matters little how the candidates are distributed among the IHLS instances, because the reduction steps performed after the candidates are selected are conservative: they will never discard one of the “good” answers once it is retrieved. Either Multi- or Hypercurves will only miss a correct answer if they fail to retrieve it from the subindexes. Therefore, Hypercurves can be made guaranteedly at least as good as Multicurves by employing on each IHLS filter copy the same probe-depth used on the sequential Multicurves. However, that is costly, and, as we will shortly see, over-pessimistic.

Consider the same database, either in a Multicurves’ subindex with probe-depth = 2Φ , or partitioned among ℓ Hypercurves’ IHLS filter copies, each with probe-depth = 2φ (even probe-depths make the analyses more symmetric, although the argument is essentially the same for odd values). For any query, the candidates that would be in a single sorted list in Multicurves are now distributed among ℓ sorted lists in Hypercurves. In more general terms, we start with a single sorted list and retrieve the 2Φ elements closest to a query vector. If we distribute randomly that single sorted list into ℓ sorted lists, how many elements must we retrieve from each of those new lists (i.e. which value for 2φ must we employ) to ensure that none of the originally retrieved elements is missed? Note that: (i) due to the sorted nature of the list, the elements before the query cannot exchange positions with the elements after the query; (ii) no element of the original list can be lost as long as all those 2ℓ “half-lists” are shorter than φ . Those observations, which are essential to understand the equivalence proof, are illustrated in Figure 7.

Due to (i), we can analyze each half of the list independently. The distribution of the elements among the ℓ lists is given by a Multinomial distribution with Φ trials and all probabilities equal to ℓ^{-1} . The exact probability of no list being longer than φ involves computing a truncated part of the distribution, but the exact formulas are exceedingly complex and little

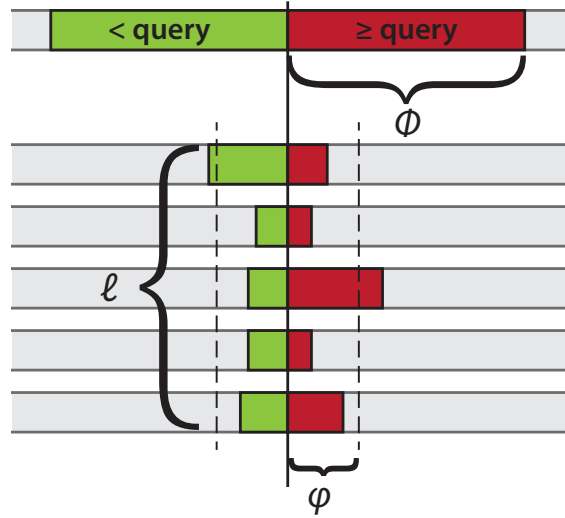


Fig. 7 The probabilistic equivalence between Multi- and Hypercurves corresponds to the following model. In a sorted list, for the query q , we retrieve Φ elements $< q$ and Φ elements $\geq q$. If we distribute the elements of that list randomly into ℓ sorted lists, how many 2φ elements must we retrieve in each of those new lists, in order to ensure missing none of the original ones. Because the elements $< q$ and $\geq q$ cannot exchange positions, each “half-list” can be analyzed independently. In the example shown, the equivalence is not guaranteed, because some elements “spill over” the φ limit in two of the half-lists.

elucidative. We can, however, bound it from below [36] with:

$$P(List_{max} \leq \varphi) \geq 1 - (\Phi \times P(List_i > \varphi)) \quad (5)$$

where $List_i$ is an arbitrary single component of the equiprobable Multinomial, which, by construction has a Binomial distribution for Φ trials and success rate of ℓ^{-1} . Thus, the probability of any miss on any of the 2ℓ half-lists is bounded from above by:

$$\begin{aligned} 1 - \text{Max} \left[0; 1 - \Phi \sum_{k=\varphi+1}^{\Phi} \binom{\Phi}{k} \left(\frac{1}{\ell}\right)^k \left(1 - \frac{1}{\ell}\right)^{\Phi-k} \right]^2 \\ = 1 - \text{Max} [0; 1 - \Phi (1 - I_{1-\ell^{-1}}(\Phi - \varphi, \varphi + 1))]^2 \end{aligned} \quad (6)$$

where $I()$ is the regularized incomplete Beta function. That probability tends to zero for very reasonable values of φ , still much lower than Φ . That is more easily seen if we make $\varphi = (1 + \varsigma) \lceil \Phi/\ell \rceil$, i.e., if we “distribute” the probe-depth among the filters, adding a “slack factor” of ς . For all reasonable scenarios, the

probability tends to zero very fast, even for small ς (Figure 8).

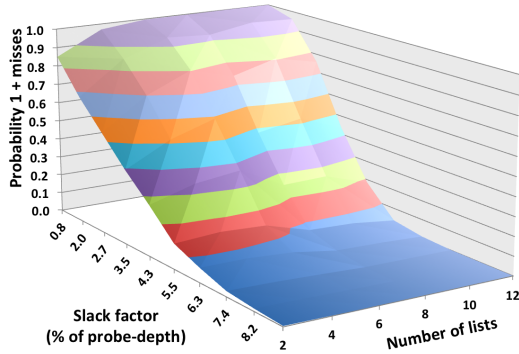


Fig. 8 Equivalence between sequential Multicurves with a probe-depth of $2\Phi = 256$ and parallel Hypercurves with distributed probe-depth of 2φ , with $\varphi = (1 + \varsigma) \lceil \Phi/\ell \rceil$ and $\ell =$ the number of filter copies. The probability of missing any of the candidate vectors drops sharply to zero, for values of ς that are still very small.

5 Hypercurves in Heterogeneous CPU–GPU Environments

The use of GPUs as general computing processors is a strong trend in high performance computing, and represents a major paradigm shift towards massively parallel and power efficient systems. GPUs have an impressive computing power, but taking advantage of them is challenging, especially for online services like Hypercurves.

In this section, we introduce the design and implementation of Hypercurves for heterogeneous, CPU–GPU environments, with a set of optimizations to maximize its performance. We anticipate that the use of GPUs in this context raises important challenges, especially in what concerns the optimization of response times under fluctuating request loads. Those dynamic aspects are discussed in Section 6.

5.1 GPU-based IHLS Implementation

In the Hypercurves pipeline, the IHLS filter is responsible for performing the compute-intensive operations of the application. Consequently, it is the phase of Hypercurves to be accelerated using GPUs. The computation performed by IHLS has granularity per user request (query), and the query execution depends

on the probe-depth (the number of candidates returned from the subindexes for further kNN computation, explained on Section 3.1) as the distances from the query to all candidates are calculated.

However, a single query is insufficient to fully utilize a GPU, because probe-depths assume small values, around a few hundred elements. Therefore, the first step towards using GPUs to accelerate this filter was to modify IHLS to group an arbitrary number of queries (**group-size**), which are then dispatched together for execution in a GPU. Our parallelization uses the CPU to perform the operations related to query grouping, while the GPU is employed during the kNN search. The execution of the IHLS filter is divided into stages (Figure 5.1–a), explained below:

Retrieve candidates: returns the probe-depth vectors closest to the query from each subindex (Lines 3 to 8 in Algorithm 2). Those candidates are accumulated in a continuous block of memory (the *CPU buffer*). That operation is repeated for each query in the group. At the end, the buffer will contain group-size sets of candidates, each set with probe-depth vectors.

Copy to GPU buffer: copies the buffer from the system memory (*CPU buffer*) to the GPU memory (the *GPU buffer*);

Perform kNN search: computes the kNN search for all group-size sets of candidates in parallel, comparing each query to its own candidate set. At the end, returns the results in *kNN results*, which will have group-size sets, each with k answers;

Send to aggregator: copies the results sets from the GPU memory and sends them downstream to the Aggregator filter, which is the next stage in processing pipeline.

The operation performed in *retrieve candidates* is a binary search on each subindex, with very irregular access patterns, dependent on both the query and the database. Since it is not realistic to assume that an entire subindex would fit into the GPU memory, the implementation of that stage in the accelerator is not worthwhile: it would require intensive data transfer between CPU and GPU. Fortunately, its computational cost is low, due to the logarithmic growth of the binary search with respect to database size. It can be executed fairly efficiently on CPU.

Perform kNN search is a special version of the traditional kNN, which compares several

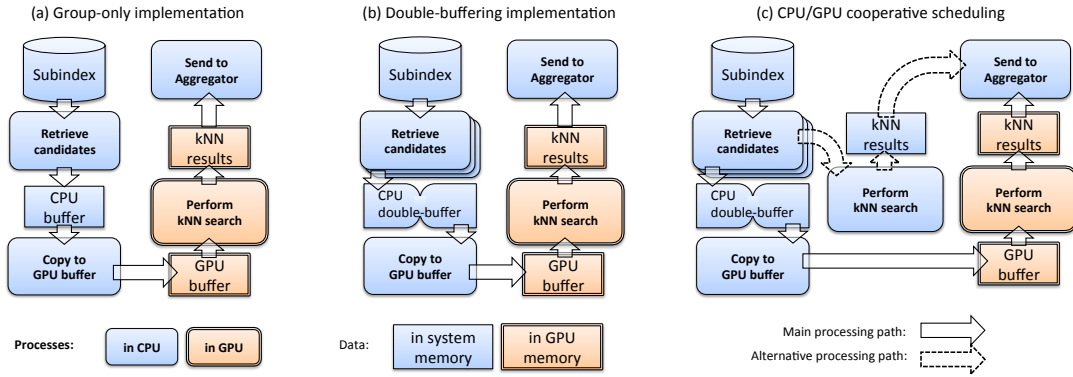


Fig. 9 The three progressively sophisticated proposed schemes for implementing Hypercurves in CPU–GPU heterogeneous environments. (a) Grouping queries to fully utilize the GPU. (b) Additionally, employing a double-buffer to avoid idleness either on CPUs and GPU. (c) Additionally, using CPUs unutilized capacity to perform kNN in an alternative processing path.

queries against the same database [24]. Here, however, each query is independently compared to a different subset of the data, which consists of the candidates just retrieved from the subindexes. In addition, the number of queries available to execute (group-size) will vary between executions. The group-size can be optimized according to a metric of interest, for instance, average response time as is detailed in the following sections.

The kNN search itself is implemented using two GPU computing *kernels*: (i) *CalcDist*, which calculates the distance between each query and its candidates; (ii) *FindTopK*, which selects the k nearest vectors among the candidates, and moves them to the top positions in the list.

The other operations, *copy to GPU buffer* and *send to aggregator* involve data transfers between the system memory and the GPU memory. The latter also involves dispatching the results for further processing downstream, in the Aggregator filter.

5.2 Overlapping CPU and GPU phases

In the design just discussed, the IHLS steps are performed sequentially, resulting in no overlapping between CPU and GPU computations. However, this approach creates idle periods in both devices. The GPU has to wait until its data buffers are filled by the CPU with the candidates retrieved from the subindexes; and the CPU has to wait until the kNN execution is completed on the GPU to transfer the next batch.

In order to reduce idleness, we propose to overlap those operations by pipelining them and using a double-buffer scheme for the communication between operations composing the IHLS filter (Figure 5.1–b). It then allows the CPU to accumulate the sets of candidates from incoming queries, while the GPU may be asynchronously processing the kNN search for the previous batch of queries. Additionally, this design employs several CPU threads to retrieve candidates from the subindexes in parallel. That strategy significantly reduces Hypercurves execution times, because it maximizes the utilization of the GPU.

Similar double-buffer schemes [46] have been used in multi-core CPU architectures, for instance, to overlap useful computation with data transfers among different levels of the memory hierarchy. Here, on the other hand, it is employed to enable pipelining and, consequently, to overlap execution of different code sections on different devices of the hybrid environment.

5.3 Cooperative execution on CPU and GPU

In the design of Hypercurves described so far, the CPU cores perform only operations which are not appropriate for GPUs: the retrieval of candidates, the data transfers, and the task of coordinating the GPU execution. However, as discussed, the cost of those CPU computations is low, and may not be sufficient to completely occupy all CPU cores available, especially in current multi-core architectures. To better utilize the CPUs, we propose to employ them also

to perform the kNN computations. However that must occur only when they would otherwise be idle, meaning that the next buffer with query candidates is ready for the GPU execution.

In our cooperative CPU/GPU scheduling solution (Figure 5.1-c), the CPU execute both its ordinary tasks (main processing path) and the kNN search (alternative processing path), giving the former higher priority. Thus, the CPU will follow the first path until the buffers used by the GPU are completely full, becoming afterwards available to process queries on the second path. The double-buffering scheme employed reduces the possibility of the GPU be kept waiting: even when the CPU is momentarily held on kNN search tasks, as the CPU will usually have enough time to fill the next buffer before the GPU is done with the current one.

The use of hybrid CPU-GPU computation, as well as the task scheduling problem that arises of employing those processors, has received increasing attention in the last few years [15, 34, 26, 31, 53, 54, 25, 43, 14]. Those works, however, assume that implementations of all stages of the computation are available for both devices, and try to minimize the execution times by employing CPU-GPU tasks partition using either static offline [26, 15, 34] or online [53, 43] strategies. Those strategies may work well in several contexts, including ones with divisible workloads, such as generalized reductions or MapReduce computations. However, they are restricted to cases where both CPU and GPU implementations are available for each stage. That contrasts to Hypercurves, where the CPU is used to assist the GPU in tasks that are not appropriate for acceleration, besides perform its own compute-intensive tasks during periods of idleness. Therefore, Hypercurves' task partitioning has to assign dynamically the priorities to types of tasks the CPU performs.

The next sections will further elaborate on that problem of task partition to minimize response times in online applications. To the best of our knowledge, ours is the first work to address that problem on CPU-GPU computation environments.

6 Response Time Aware Task Partition in Heterogeneous CPU-GPU Platforms

As discussed, the online nature of Hypercurves poses the interesting challenge of optimizing

the response time of the individual queries, while using GPUs, which are throughput-oriented devices. In order to reduce response times, it is necessary to perform a dynamic partition of the load among CPU and GPU under a fluctuating user request load. That partition in Hypercurves is directly related to the group-size used by IHLS, which will determine the number of tasks queued for GPU execution and, consequently, those remaining for CPU computation. The optimal configuration for each load intensity depends on complex factors, including the hardware architecture, application parameters, and dataset properties. Such complex optimization is beyond the ability of any static configuration.

Formally, the problem can be defined as such: given a set of n tasks $t_1 \dots t_n$ within a filter, m processors $p_1 \dots p_m$ allocated to that filter, the execution time of each task in each processor denoted by e_{ij} , and the wait time of each task to be processed by each processor as w_{ij} , we want to determine the schedule x_{ij} where $1 \leq i \leq n$ and $1 \leq j \leq m$. Each x_{ij} is a binary variable indicating whether the tasks i is executed by processor j . Notice that, for a given task t_i , there exists just one x_{ij} , $1 \leq j \leq m$ that is nonzero. Since there is no task reordering within a processor, the w_{ij} is defined as the sum of the processing time of tasks e_{xj} computed by a given processor j before it gets to execute x .

Our goal is to find a schedule that minimize E , the average execution time of the tasks within each application filter. For simplicity, and since the filters execute independently, we state the problem in terms of a single filter. In general, the execution time takes the form:

$$E = \text{avg}_{i=0\dots n} \sum_{j=1}^m x_{ij} \times (e_{ij} + w_{ij}) \quad (7)$$

The execution time e_{ij} varies according to the processor used. For the GPU, it has two components: a buffer-waiting time, in which the task remains buffered in the CPU memory; and the computation, which involves both the data transfer between CPU and GPU, and the execution itself. The cost of both components further depends on the task granularity (group-size).

Scheduling in such environment is difficult for various reasons: (i) the problem is NP-hard, since the bin packing problem, widely known to

be NP-hards, is a very simplified version of the scheduling problem discussed (the equivalence is true when waiting times are zero); (ii) the tasks are created at run time, making static scheduling impossible; (iii) estimating the execution time (e_{ij}) of a task has been an open challenge for decades [29].

The optimization is not only complex, but also dynamic, varying instantaneously as the request load changes. Thus, exact solutions would be too costly to be practical. We propose instead a light, greedy algorithm that calculates the scheduling throughout the execution, optimizing the granularity of tasks assignment to GPU (group-size), and the tasks assignment between CPU and GPU.

The solution we propose is driven by the idea that GPU use is advantageous only when the aggregate throughput delivered by the available CPU computing cores is insufficient to promptly process the demand. That approach diverges from the usual parallelizations for heterogeneous environments, where GPUs are systematically preferred for their capacity to achieve highest throughputs. However, as discussed before, the use of GPUs improve throughput at the cost of increasing the average tasks processing time.

Therefore, it is not worthwhile using GPUs in online application unless the tasks response times are dominated by waiting time, which occurs when the request rates submitted to the system are above the CPU throughput. On the other hand, under high request loads, it becomes beneficial using GPUs to increase the system throughput: though the processing time of a single task will be higher, due to the overheads of starting up a GPU computation, the average response times of the system will be reduced, because the better throughput will lower or even eliminate waiting times.

The solution we propose is called Dynamic Task Assigner for Heterogeneous Environments (DTAHE) and is presented in Algorithm 3. The DTAHE is executed in parallel with the computing threads in each filter copy, and loops until the upstreams filters notify that execution has finished — the *EndOfWorks* message. Line 2 of the algorithm will check the number of events/requests queued in the filter (*ready*), and further decide whether the thread should follow the event processing using the CPU or the GPU (line 3).

If the GPU buffer is full or if the CPU computing cores available are enough to process all

Algorithm 3 Dynamic Task Assigner for Heterogeneous Environments — DTAHE.

Executes in parallel with the other threads, until the filter has nothing else to process (*EndOfWorks* becomes true). There is one independent instance of this thread for each transparent copy of each filter.

EndOfWorks: true if this filter copy has no more processing to do, false otherwise

CC: number of CPU cores allocated to this filter copy

NumEvents: the number of events waiting to be processed

GetNextEvent(): pops from the waiting queues the next event to be processed

CurrentBuffer: current GPU buffer, the one being prepared

ProcessInCPU(e): dispatches the event e to be processed in the CPU

BufferEvent(e, b): stores the event e to be processed in the buffer b

IsGPUIdle: true if the GPU is idle, false otherwise

IsFull(b): returns true if the buffer b specified is full, false otherwise

QueueInGPU(b): queue the buffer b to be processed in the GPU

```

1: while not EndOfWork do
2:   ready  $\leftarrow$  NumEvents
3:   if ready  $\leq$  CC or CurrentBuffer is full
4:     then
5:       ProcessInCPU(GetNextEvent())
6:     else
7:       event  $\leftarrow$  GetNextEvent()
8:       BufferEvent(event, CurrentBuffer)
9:       ready  $\leftarrow$  NumEvents()
10:      if (ready  $<$  CC and IsGPUIdle) or
          IsFull(CurrentBuffer) then
          QueueInGPU(CurrentBuffer)

```

queued events, an event is dequeued and dispatched to the CPU (line 4). Otherwise, an event is dequeued, the items to be compared to that query are retrieved from the subindexes and stored in the GPU data buffer (Lines 6–7). The scheduler decides, then, if the buffer should be sent for the execution in the GPU, which happens when it becomes full, when the GPU becomes idle (which we want to avoid), or if the number of ready events becomes low enough so that the remaining ones can be processed in the CPUs. Each GPU has one CPU computing core reserved for managing purposes (coordination, buffer copying, etc.), but, when that GPU has no buffers ready to be processed, its dedicated CPU core become available to perform other tasks. The motivation, again, is to get the GPU running as often and as early as possible, avoiding as much as possible to keep it waiting, while keeping the CPU available to process some queries when the GPU is busy.

DTAHE solves at once the problem of dynamically distributing the tasks among CPUs and GPUs and determining the optimal group-size. The latter is done implicitly, as buffers are dispatched for GPU computation either when they are full (maximum group-size, corresponding to situations of high loads and maximum throughput) either when the GPU becomes idle (smaller group-sizes, as the load becomes lighter). When the load becomes light enough to be dealt with just the CPU cores, the GPU is not employed, again keeping response times as short as possible. On the other hand, as the load increases, processing migrates increasingly to the GPU.

The problem of optimizing group-sizes is similar to optimizing the parallelism granularity in parallel loops or *doall*-like operations, which have been extensively studied [12]. Most works on that area, however, focus on applying loop transformations according to the available resources, in order to adjust the granularity, reducing the synchronization overhead and do not take into account load variability. The best parallelism is often beyond any static tuning. That has motivated several recent works, which focus on runtime transformations [2, 5, 17]. Those interesting works aim at parallelism tuning for a lower level and are only concerned with CPU-based machines, thus being complementary to the strategy we propose.

7 Experimental results

In this section, we evaluate the impact of our propositions on Hypercurves’ performance. The experiments have been performed using two setups of machines. The first setup consisted of 2 PCs connected through a Gigabit Ethernet, each with two quad-core AMD Opteron 2.0 GHz 2350, 16 GB of main memory, and one NVidia GeForce GTX260 GPU. The second setup was a 8-node cluster connected with Gigabit Ethernet, each node being a PC with two quad-core hyper-threaded Intel Xeon E5520, 24 GB of main memory, and one NVidia GeForce GTX470. All machines run Linux.

The main database used to evaluate our algorithm contained 130,463,526 SIFT local feature vectors [33], with 128 dimensions each. Those feature vectors have been computed from 233,852 background images from the Web, and 225 foreground images from our personal collections. The foreground images have been used to compute sets of feature vectors that

must be matched, while the background images have generated the feature vectors used to confound the method. The foreground images, after strong transformations (rotations, changes in scale, non-linear photometric transformations, noise, etc.) have also been used to create 187,839 query feature vectors. Due to the number of evaluations performed, we have also employed smaller partitions of that main database, in order both to achieve feasible experimentation running times, and to emphasize certain aspects (e.g., overhead) in specific experiments.

The experiments concentrate on issues of efficiency, since, as demonstrated in Section 4.2, Hypercurves, with very high probability, has the same results of Multicurves. Thus, by construction, it inherits the good trade-off between precision and speed of Multicurves [60].

7.1 The Impact of Task Granularity

As discussed in Section 5.1, task granularity has an important impact on the GPU acceleration achieved. In Hypercurves, it is dictated by the group-size: the number of queries aggregated to be processed concurrently within each GPU execution (Section 5.1).

This study has employed a subsample of 1,000,000 feature vectors randomly selected from the main database, and 30,000 queries. A smaller dataset has been used in order to provide shorter execution times, which are more appropriate to highlight any potential overheads in our solution. The entire set of queries has been dispatched to the filter QR at the beginning of the execution, creating a high number of concurrent queries ready to execute in the IHLS filter throughout execution (check the filter enchainment in Figure 6). In addition, in this initial evaluation, a single machine has been employed.

Figure 10 presents Hypercurves throughput (in queries per second), for 3 typical choices of probe-depth, as group-size varies up to the limit of queries that can be accommodated within the GPU memory. Group-size is kept fixed during each single execution. We focus on the impact of task grouping, expressed on the “Grouping only” curves in the graphs. The other results presented in the same graphs are discussed on the following sections.

As expected, a small number of queries is insufficient to completely utilize the GPU,

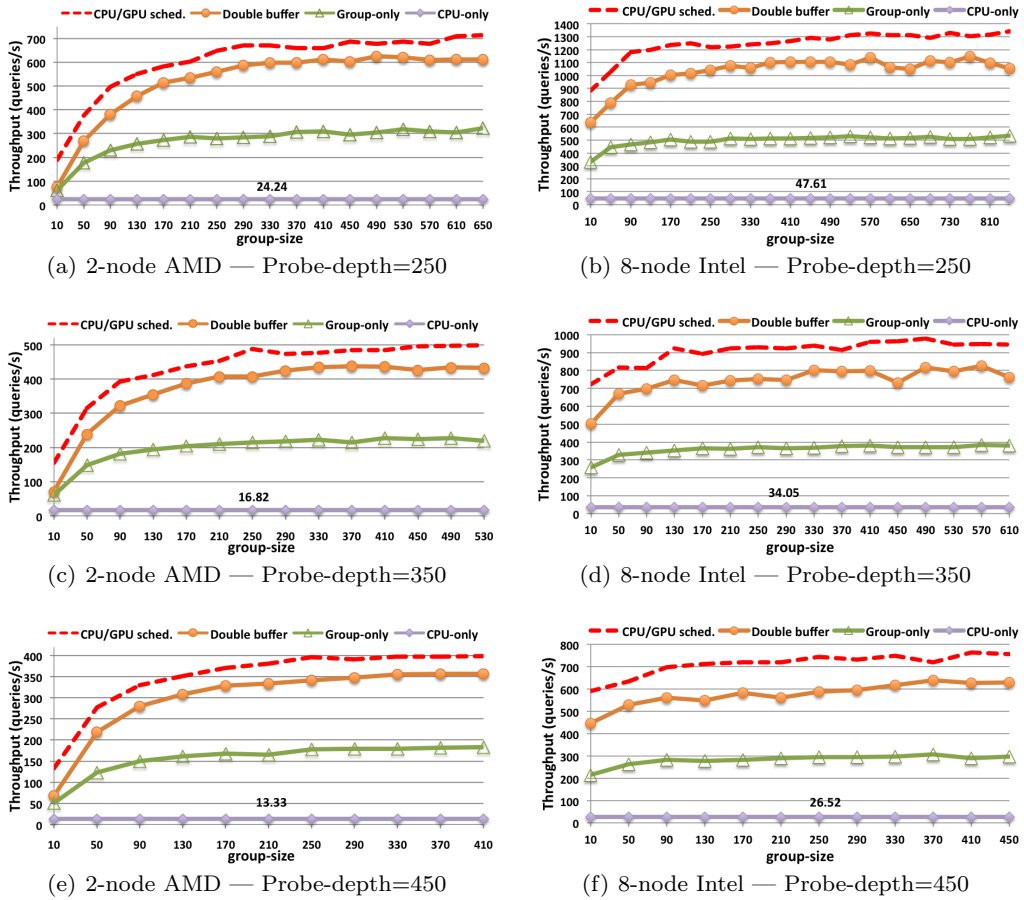


Fig. 10 Hypercurves performance as group-size varies, for multiple probe-depth values, in both machine configurations (2 nodes of AMD/GTX260, and 8 nodes of Intel/GTX450). Dynamic scheduling is *not* employed in those experiments: the parameters are kept fixed on each execution (each data point). The speedup brought by the use of the GPU is dramatic, and each successive improvement (from group-only to double-buffering to cooperative CPU/GPU scheduling) is considerable.

but the GPU performance is consistently improved as group-size increases. Also, when 50% of the maximal group-size is employed, the speedups achieved are about 90% of the best acceleration. In addition, the best speedups are similar for all probe-depths: $13.34\times$ (probe-depth=250), $13.52\times$ (probe-depth=350), and $13.73\times$ (probe-depth=450). The small impact of the probe-depth over the speedup is an important, positive property of the method, since it allows the user to calibrate that parameter more or less freely, provided that there are enough queries to group and process in parallel.

The gains attained by task grouping are promising, enhancing a very efficient approximate search algorithm — whose sequential CPU implementation is already orders of magnitude faster than the exact search. In the following sections, we will demonstrate increasing performance gains, obtained by the optimiza-

tions proposed on top of that GPU parallelization (See Section 5).

7.2 The Effect of Overlapping CPU and GPU

Figure 10 presents the performance of Hypercurves when using the double-buffering scheme intended to maximize the GPU utilization by reducing the waiting time between batches of queries. That enhancement, discussed in Section 5.2, is built on top of the grouping mechanism demonstrated in the previous section. The results are shown in the curve labeled “Double buffer”.

Similarly to the “Grouping only” case, the performance grows as the value of group-size increases, nearly doubling the throughput of the grouping-only version for most of the group-size values. When compared to the single CPU

core execution, the maximum speedups of the double-buffered GPU-accelerated version are 25.81, 26.02, and 26.75, for probe-depths 250, 350, and 450 respectively.

During the evaluation, a complete overlapping of the CPU and the GPU was achieved, except at the very beginning, during the preparation of the first batch of queries. We have also observed that, in all experiments, the GPU was always occupied processing queries, while the CPU experienced idle periods for the threads responsible for retrieving candidates from the subindexes and copy them to the buffers. The CPU underutilization motivated its use in the kNN phase of the application, in addition to the preparation of the buffers for the GPU. That cooperative strategy is evaluated in the next section.

7.3 Maximizing CPU–GPU Cooperation

Since the CPUs present in our systems prepare the buffers faster than the GPU is able to consume them, they experience idle periods. To maximize the system performance under those circumstances, we also employed the CPU cores in the compute-intensive kNN tasks during that idleness, as discussed in Section 5.3. In the remainder of this section, the benefits of that strategy are evaluated in addition to double-buffering and grouping. Figure 10 shows the results, in the curves labeled “CPU/GPU sched.”.

As shown, the gains with that technique are very relevant, and speedups of $1.23\times$, $1.22\times$ and $1.22\times$ for, respectively, probe-depths of 250, 350 and 450 were achieved on top of the previous version of Hypercurves.

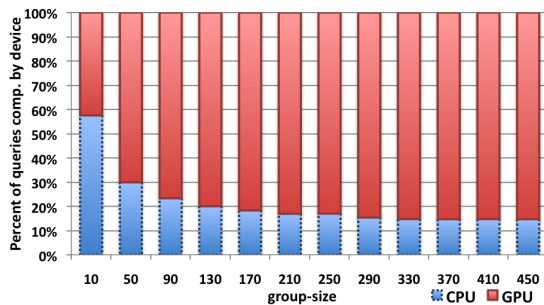


Fig. 11 Fraction of the tasks computed by each type of device (CPU vs. GPU) as group-size varies, illustrating how GPU utilization is favored by large group-sizes. Those experiments were executed on an AMD node using probe-depth of 350.

Interestingly, the speedup obtained here slightly decreases as the group-size increases. This behavior is consequence of the higher efficiency of the GPU for large group-sizes, which tends to reduce the idle time of the CPU cores. Figure 11 illustrates that as the group-size grows, more queries tend to be processed by the GPU instead of the using CPU for the kNN phase. Even so, the improvements achieved were rewarding, with more than $1.2\times$ average speedup across the group-size configurations used. As the number of available CPU cores also tend to increase in new architectures, the potential of using those devices in cooperation with the GPU cannot be neglected.

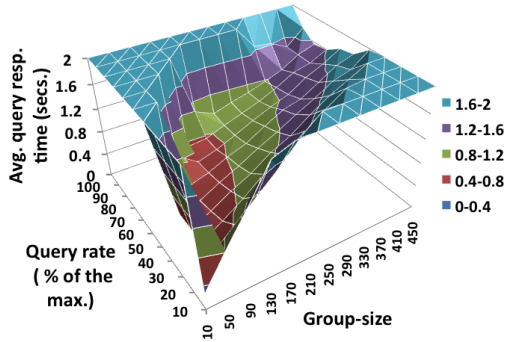
7.4 Granularity vs. Response Times

So far, in the experimental evaluation, we have analyzed Hypercurves performance in scenarios where a very large number of queries is submitted at once, thus assessing the application throughput capabilities. However, in real-world operation, the query rate submitted to an on-line application is generated by users, and is subjected to variability throughout the execution. Moreover, under those circumstances, the most important metric is the response time observed by the users. Therefore, in this section, we analyze how the grouping technique and cooperative CPU–GPU execution impact the average query response time.

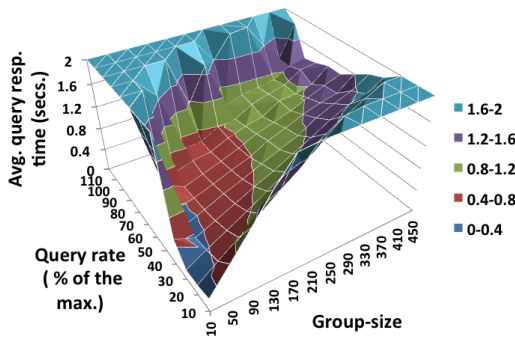
In this analysis, we vary both the number of queries submitted per second and group-size across experiments, but *keep them fixed within each run*. The capacity of adjusting the group-size dynamically is evaluated in the next section.

We employ the same 1,000,000-vectors database, and the 30,000 queries used in previous sections. First, in Figure 12(a), we present the average response times of Hypercurves when the GPU is used to compute all the tasks, and the group-size is varied.

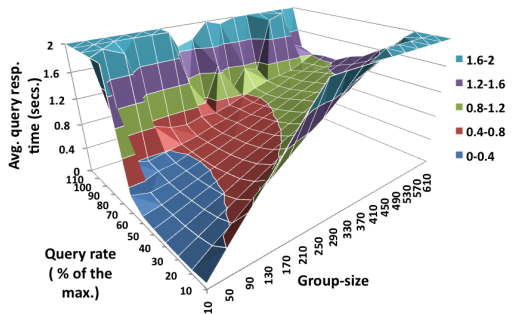
It is noticeable that a single, fixed, group-size value is unable to deliver the best response times for all request loads. The response-time function we seek to optimize has a complex behavior and its minimum moves up the group-size axis as the query rate increases. Hypercurves has been able to answer queries in reasonably low response times until the load reached about 80% of the maximum supported by the configuration, but after that point response times have grown steeply.



(a) 2-node AMD — GPU-only



(b) 2-node AMD — CPU-GPU



(c) 8-node Intel — CPU-GPU

Fig. 12 Average query response times as query rate (% of the maximum) and group-size vary, for a probe-depth of 350. The parameters are kept fixed on each execution (each data point). The graphs demonstrate the complex task of optimizing group-size as the load (query-rate) fluctuates.

The comparison of Hypercurves using only the GPU for kNN, versus the cooperative CPU-GPU configuration is possible contrasting Figures 12(a) and 12(b). Visual inspection of those figures show that the CPU-GPU cooperation resulted in a systematic reduction of the average response times. Moreover, across all the experiments, the CPU-GPU version reduces the response times in 58%, on average.

Those gains are much more impacting that the previous improvements in throughput achieved with the same cooperation (Section 7.3). The reason is that although the CPU has a lower throughput, the response times of the queries processed by this device are much smaller: the queries routed to the GPU have a longer processing path, having to be queued, copied to the GPU, processed using lower frequency cores, and copied back to the system main memory.

We also present the performance of Hypercurves using CPU-GPU collaboratively for the Intel/GTX470 node in Figure 12(c). When compared to the AMD/GTX260 machine, the performance of the Intel node is superior, and much better average response-times are achieved. That is mainly a consequence of the improvements in design achieved by the GTX470 GPU as compared to the GTX260 GPU, as the first has more computing cores, better bandwidth, etc.

7.5 Response times on variable request rates

In this section, we analyze the DTAHE dynamic scheduler (Section 6) capacity to adapt Hypercurves' work partition among CPU and GPU under scenarios with stochastically variable workloads. During this evaluation, the load/request rate follows a Poisson distribution, with expected average rate (λ) varying from 20 to 100% of the maximum throughput of the application in each configuration. That maximum throughput is computed in a preliminary run, where all the queries are sent for computation in the beginning of the execution. This set of experiments employ the cooperative CPU-GPU computation, and a probe-depth of 350.

The results are summarized in Table 1. The best static configuration refers to the minimum response times achieved from an exhaustive search in the group-size space for each query rate employed. It is noticeable that DTAHE strongly outperform the best static configuration for most of the cases. On average, its response times are 52% (2-node AMD) and 81% (8-node Intel) of the best static configuration.

The only configurations where DTAHE falls slightly behind static scheduling have Poisson rates λ equal to 100% of the maximum throughput bearable by the machines. In that extreme scenario not much can be accomplished by dynamic scheduling, since the goal of maximum throughput coincides with the one of minimum

(a) First setup (2-node AMD)					
Scheduling	Poisson λ (% of max. throughput)				
	20	40	60	80	100
Best static	0.11	0.4	0.42	0.61	0.98
DTAHE	0.06	0.13	0.14	0.22	1.02

(b) Second setup (8-node Intel)					
Scheduling	Poisson λ (% of max. throughput)				
	20	40	60	80	100
Best static	0.054	0.098	0.12	0.25	0.65
DTAHE	0.034	0.089	0.1	0.16	0.68

Table 1 Average query response times (in s) for static and dynamically-tuned scheduling configurations, under stochastic loads. Unless the system is completely saturated, the dynamic scheduling always wins, usually by a considerable margin.

response times, and a simple static configuration manages that with slightly less overhead. The differences, however, are small, and dynamic scheduling is, of course, much more flexible.

7.6 Evaluating Hypercurves’ scalability

The distributed memory analysis in this section has focused on evaluating Hypercurves scaleup. We consider the compromises between performance of the parallelism and conservation of the results precision, as the database is partitioned among the computing nodes. The scaleup evaluation is appropriate in our application scenario because we expect to have an abundant volume of data for indexing, thus the speedup evaluation starting with a single node holding the entire database might not be realistic. The experiments executed in this section used the 8-node Intel cluster, employing all CPU cores and GPUs available on the nodes. The main database with 130,463,526 local feature vectors is used proportionally, with $n/8$ of the database being used for the experiment with n nodes.

The query rate delivered by the algorithm considers two parameterization scenarios named Optimist and Pessimist (Table 2), which differ in their guarantees of equivalence (in terms of precision of the kNN search) to the sequential Multicurves algorithm. The Optimist parameterization divides the probe-depth equally among the nodes, without any slack — it will only be equivalent to Multicurves in the unlikely case that all candidates of that query are equally distributed on the nodes. The Pessimist parameterization uses a slack that guarantees a probability smaller than 2% that a

candidate vector selected by the sequential algorithm will be missing from the distributed version (see Section 4.2 for details). Note that that choice is extremely conservative, because in order to effectively affect the answer, the missed feature vectors from the candidate set have to be among the actual top- k set, and k is much smaller than the probe-depth.

Table 2 presents Hypercurves query rates on the scaleup evaluation. As shown, the scalability of the algorithm is impressive for both Optimist and Pessimist configurations, achieving *superlinear scaleup* in all setups. That strong performance of Hypercurves is observed because the application is only affected by the size of the database during the phase where candidates are retrieved from subindexes and the cost of that stage grows only logarithmically with the size of the database. The costly phase of computing the distances from the query to the retrieved candidates can, thanks to the probabilistic equivalence (Section 4.2), be efficiently distributed among the nodes, with a relatively small overhead.

Not only is the scalability of the algorithm very good, but its raw response rates (queries per s) are very high. For instance, number of queries that the algorithm would be able to answer a per day are: 646 and 443 million, respectively, for the Optimist and the Pessimist configurations. Those rates indicate that by employing the technology proposed, a large-scale image search system could be built at reasonably low hardware and power costs per request, since GPU accelerators are very computational- and power-efficient platforms.

Number of nodes	1	2	3	4	5	6	7	8
# of cores / # of GPUs	16 / 1	32 / 2	48 / 3	64 / 4	70 / 5	86 / 6	102 / 7	118 / 8
Optimist — queries per s	964	1904	2649	3598	4490	5397	6297	7483
Pessimist — queries per s	964	1683	2197	2849	3416	3968	4498	5135

Table 2 Scaleup evaluation: query rate as database and number of nodes increase proportionally (probe-depth=350).

8 Conclusions and future work

This work has proposed and evaluated Hypercurves, an online similarity search engine for very large multimedia databases. Hypercurves has been designed to fully exploit massively parallel machines, with both CPUs and GPUs. Its use in a CPU-GPU environment, along with a set of optimizations, resulted in accelerations of about 30× on top of the single-core CPU version.

We have also studied the problem of response-time aware (DTAHE) partition of tasks between CPU and GPU, under request load fluctuations, which occurs as a result of the varying number of queries submitted by the user to the application. DTAHE has been able to reduce the average query response times in about 50% and 80% (respectively for both machine configurations used in the experiments), when compared to the best static partition in each case. Furthermore, Hypercurves achieved *superlinear* scaleups in all experiments, while keeping a high guarantee of equivalence with the sequential Multicurves algorithm, as asserted by the proof of probabilistic equivalence.

We are currently interested in the complex interactions between algorithmic design and parallel implementation for services such as Hypercurves. We are also investigating how a complete system for content-based image retrieval can be built upon our indexing services, and optimized using our techniques and scheduling algorithms. We consider it a promising direction for future, as Hypercurves subindexes implementation in heterogeneous environments offers very good reply rate.

References

1. Akune, F., Valle, E., Torres, R.: Monorail: A disk-friendly index for huge descriptor databases. In: 2010 20th International Conference on Pattern Recognition (ICPR), pp. 4145–4148 (2010). DOI 10.1109/ICPR.2010.1008
2. Aleen, F., Sharif, M., Pande, S.: Input-driven dynamic execution prediction of streaming applications. In: Proc. of the 15th ACM SIGPLAN symposium on Principles and practice of parallel programming, PPOPP '10. ACM (2010)
3. Beynon, M., Ferreira, R., Kurc, T.M., Sussman, A., Saltz, J.H.: DataCutter: Middleware for filtering very large scientific datasets on archival storage systems. In: IEEE Symposium on Mass Storage Systems, pp. 119–134 (2000)
4. Bhatti, N.T., Hiltunen, M.A., Schlichting, R.D., Chiu, W.: Coyote: a system for constructing fine-grain configurable communication services. ACM Trans. Comput. Syst. **16**(4), 321–366 (1998). DOI 10.1145/292523.292524
5. Blagojevic, F., Nikolopoulos, D.S., Stamatakis, A., Antonopoulos, C.D., Curtis-Maury, M.: Runtime scheduling of dynamic parallelism on accelerator-based multi-core systems. Parallel Comput. **33**, 700–719 (2007). DOI 10.1016/j.parco.2007.09.004
6. Böhm, C., Berchtold, S., Keim, D.A.: Searching in high-dimensional spaces: Index structures for improving the performance of multimedia databases. ACM Comput. Surv. **33**, 322–373 (2001). DOI 10.1145/502807.502809
7. Boureau, Y.L., Bach, F., LeCun, Y., Ponce, J.: Learning mid-level features for recognition. Computer Vision and Pattern Recognition, IEEE Computer Society Conference on **0**, 2559–2566 (2010). DOI 10.1109/CVPR.2010.5539963
8. Butz, A.R.: Alternative algorithm for hilbert's space-filling curve. IEEE Trans. on Computers **C-20** (1971)
9. Castelli, V.: Multidimensional Indexing Structures for Content-Based Retrieval, pp. 373–433. John Wiley & Sons, Inc. (2002). DOI 10.1002/0471224634.ch14
10. Chandrasekhar, V., Sharifi, M., Ross, D.A.: Survey and evaluation of audio fingerprinting schemes for mobile query-by-example applications. In: A. Klapuri, C. Leider (eds.) ISMIR, pp. 801–806. University of Miami (2011)
11. Chávez, E., Navarro, G., Baeza-Yates, R., Marroquín, J.L.: Searching in metric spaces. ACM Comput. Surv. **33**(3), 273–321 (2001). DOI 10.1145/502807.502808
12. Chen, D.K., Su, H.M., Yew, P.C.: The impact of synchronization and granularity on parallel systems. SIGARCH Comput. Archit. News **18**, 239–248 (1990). DOI 10.1145/325096.325150
13. Datar, M., Immorlica, N., Indyk, P., Mirrokni, V.S.: Locality-sensitive hashing scheme based on p-stable distributions. In: Proceedings of the twentieth annual symposium on Computational geometry, SCG '04, pp. 253–262. ACM, New York, NY, USA (2004). DOI 10.1145/997817.997857
14. Diamos, G.F., Yalamanchili, S.: Harmony: an execution model and runtime for heterogeneous many core systems. In: Proceedings of the 17th international symposium on High performance distributed computing, HPDC '08, pp. 197–200.

- ACM, New York, NY, USA (2008). DOI <http://doi.acm.org/10.1145/1383422.1383447>
15. Ding, S., He, J., Yan, H., Suel, T.: Using graphics processors for high-performance ir query processing. In: Proceeding of the 17th international conference on World Wide Web, WWW '08, pp. 1213–1214. ACM, New York, NY, USA (2008). DOI [10.1145/1367497.1367732](https://doi.org/10.1145/1367497.1367732)
 16. Du Mouza, C., Litwin, W., Rigaux, P.: Large-scale indexing of spatial data in distributed repositories: the sd-rtree. *The VLDB Journal* **18**, 933–958 (2009). DOI [10.1007/s00778-009-0135-4](https://doi.org/10.1007/s00778-009-0135-4)
 17. Duran, A., Silvera, R., Corbalán, J., Labarta, J.: Runtime adjustment of parallel nested loops. In: B.M. Chapman (ed.) *Shared Memory Parallel Programming with Open MP*, *Lecture Notes in Computer Science*, vol. 3349. Springer Berlin / Heidelberg (2005)
 18. Fagin, R., Kumar, R., Sivakumar, D.: Efficient similarity search and classification via rank aggregation. In: Proceedings of the 2003 ACM SIGMOD international conference on Management of data, SIGMOD '03, pp. 301–312. ACM, New York, NY, USA (2003). DOI [10.1145/375757.872795](https://doi.org/10.1145/375757.872795)
 19. Fagin, R., Lotem, A., Naor, M.: Optimal aggregation algorithms for middleware. In: Proc. of the 20th ACM SIGMOD-SIGACT-SIGART Symp. on Principles of database systems, PODS '01, pp. 102–113. ACM (2001). DOI [10.1145/375551.375567](https://doi.org/10.1145/375551.375567)
 20. Faloutsos, C.: Gray codes for partial match and range queries. *IEEE Trans. Softw. Eng.* **14**, 1381–1393 (1988). DOI [10.1109/32.6184](https://doi.org/10.1109/32.6184)
 21. Faloutsos, C.: *Multimedia Indexing*, pp. 435–464. John Wiley & Sons, Inc. (2002). DOI [10.1002/0471224634.ch15](https://doi.org/10.1002/0471224634.ch15)
 22. Faloutsos, C., Roseman, S.: Fractals for secondary key retrieval. In: Proceedings of the eighth ACM SIGACT-SIGMOD-SIGART symposium on Principles of database systems, PODS '89, pp. 247–252. ACM, New York, NY, USA (1989). DOI [10.1145/73721.73746](https://doi.org/10.1145/73721.73746)
 23. Ferreira, R., Jr., W.M., Guedes, D., Drummond, L., Coutinho, B., Teodoro, G., Tavares, T., Araujo, R., Ferreira, G.: Anthill: a scalable run-time environment for data mining applications. In: *Symposium on Computer Architecture and High-Performance Computing (SBAC-PAD)* (2005)
 24. Garcia, V., Debreuve, E., Barlaud, M.: Fast k nearest neighbor search using GPU. In: *CVPR Workshop on Computer Vision on GPU (CVGPU)*. Anchorage, Alaska, USA (2008)
 25. Hartley, T.D., Catalyurek, U.V., Ruiz, A., Ujaldon, M., Igual, F., Mayo, R.: Biomedical Image Analysis on a Cooperative Cluster of GPUs and Multicores. In: *22nd ACM Intl. Conference on Supercomputing* (2008)
 26. He, B., Fang, W., Luo, Q., Govindaraju, N.K., Wang, T.: Mars: A mapreduce framework on graphics processors. In: *Parallel Architectures and Compilation Techniques* (2008)
 27. Hua, G., Fu, Y., Turk, M., Pollefeys, M., Zhang, Z.: Introduction to the special issue on mobile vision. *International Journal of Computer Vision* **96**, 277–279 (2012). DOI [10.1007/s11263-011-0506-3](https://doi.org/10.1007/s11263-011-0506-3)
 28. Indyk, P., Motwani, R.: Approximate nearest neighbors: Towards removing the curse of dimensionality. In: *STOC*, pp. 604–613 (1998). DOI [10.1145/276698.276876](https://doi.org/10.1145/276698.276876)
 29. Kerbyson, D.J., Alme, H.J., Hoisie, A., Petrini, F., Wasserman, H.J., Gittings, M.: Predictive performance and scalability modeling of a large-scale application. In: *Supercomputing '01: Proceedings of the 2001 ACM/IEEE conference on Supercomputing (CDROM)*, pp. 37–37 (2001). DOI [10.1145/582034.582071](https://doi.org/10.1145/582034.582071)
 30. Liao, S., Lopez, M.A., Leutenegger, S.T.: High dimensional similarity search with space filling curves. In: *Proc. of the 17th Int. Conf. on Data Engineering*, pp. 615–622 (2001)
 31. Linderman, M.D., Collins, J.D., Wang, H., Meng, T.H.: Merge: a programming model for heterogeneous multi-core systems. *SIGPLAN Not.* **43**(3), 287–296 (2008). DOI [10.1145/1353536.1346318](https://doi.org/10.1145/1353536.1346318)
 32. Liu, Y., Zhang, D., Lu, G., Ma, W.Y.: A survey of content-based image retrieval with high-level semantics. *Pattern Recognition* **40**(1), 262–282 (2007). DOI [10.1016/j.patcog.2006.04.045](https://doi.org/10.1016/j.patcog.2006.04.045)
 33. Lowe, D.G.: Distinctive image features from scale-invariant keypoints. *Int. J. Comput. Vision* **60**, 91–110 (2004). DOI [10.1023/B:VISI.0000029664.99615.94](https://doi.org/10.1023/B:VISI.0000029664.99615.94)
 34. Luk, C.K., Hong, S., Kim, H.: Qilin: Exploiting parallelism on heterogeneous multiprocessors with adaptive mapping. In: *42nd International Symposium on Microarchitecture (MICRO)* (2009)
 35. Mainar-Ruiz, G., Perez-Cortes, J.C.: Approximate nearest neighbor search using a single space-filling curve and multiple representations of the data points. In: *Proceedings of the 18th International Conference on Pattern Recognition - Volume 02, ICPR '06*, pp. 502–505. IEEE Computer Society, Washington, DC, USA (2006). DOI [10.1109/ICPR.2006.275](https://doi.org/10.1109/ICPR.2006.275)
 36. Mallows, C.L.: An inequality involving multinomial probabilities. *Biometrika* **55**(2), pp. 422–424 (1968)
 37. Megiddo, N., Shaft, U.: Efficient nearest neighbor indexing based on a collection of space filling curves. Tech. Rep. IBM Research Report RJ 10093 (91909), IBM Almaden Research Center, San Jose California (1997)
 38. Mikolajczyk, K., Schmid, C.: A performance evaluation of local descriptors. *IEEE Transactions on Pattern Analysis and Machine Intelligence* **27**, 1615–1630 (2005). DOI [10.1109/TPAMI.2005.188](https://doi.org/10.1109/TPAMI.2005.188)
 39. Morton, G.M.: A computer oriented geodetic data base and a new technique in file sequencing. Tech. Rep. Technical Report, IBM Ltd., Ottawa, Ontario, Canada (1966)
 40. O'Malley, S.W., Peterson, L.L.: A dynamic network architecture. *ACM Trans. Comput. Syst.* **10**(2) (1992). DOI [10.1145/128899.128901](https://doi.org/10.1145/128899.128901)
 41. Pang, H., Ding, X., Zheng, B.: Efficient processing of exact top-k queries over disk-resident sorted lists. *The VLDB Journal* **19**, 437–456 (2010). DOI [10.1007/s00778-009-0174-x](https://doi.org/10.1007/s00778-009-0174-x)
 42. Penatti, O.A.B., Valle, E., Torres, R.d.S.: Comparative study of global color and texture descriptors for web image retrieval. *J. Vis. Commun. Image Represent.* **23**(2), 359–380 (2012). DOI [10.1016/j.jvcir.2011.11.002](https://doi.org/10.1016/j.jvcir.2011.11.002)

43. Ravi, V., Ma, W., Chiu, D., Agrawal, G.: Compiler and runtime support for enabling generalized reduction computations on heterogeneous parallel configurations. In: Proceedings of the 24th ACM International Conference on Supercomputing, pp. 137–146. ACM (2010)
44. Sagan, H.: *Space-Filling Curves*. Springer-Verlag, New York, NY, USA (1994)
45. Samet, H.: *Foundations of Multidimensional and Metric Data Structures (The Morgan Kaufmann Series in Computer Graphics and Geometric Modeling)*. Morgan Kaufmann Publishers Inc., San Francisco, CA, USA (2005)
46. Sancho, J.C., Kerbyson, D.J.: Analysis of Double Buffering on two Different Multicore Architectures: Quad-core Opteron and the Cell-BE. In: International Parallel and Distributed Processing Symposium (IPDPS) (2008)
47. Shakhnarovich, G., Darrell, T., Indyk, P.: *Nearest-Neighbor Methods in Learning and Vision: Theory and Practice (Neural Information Processing)*. The MIT Press (2006)
48. Shepherd, J., Zhu, X., Megiddo, N.: A fast indexing method for multidimensional nearest neighbor search. In: SPIE Conference on Storage and Retrieval for Image and Video Databases VII, pp. 350–355 (1999)
49. Smeulders, A., Worring, M., Santini, S., Gupta, A., Jain, R.: Content-based image retrieval at the end of the early years. *Pattern Analysis and Machine Intelligence, IEEE Trans. on* **22**(12), 1349–1380 (2000). DOI 10.1109/34.895972
50. Stone, Z., Zickler, T., Darrell, T.: Autotagging facebook: Social network context improves photo annotation. In: Computer Vision and Pattern Recognition Workshops, 2008. CVPRW '08. IEEE Computer Society Conference on, pp. 1–8 (2008). DOI 10.1109/CVPRW.2008.4562956
51. Teodoro, G., Fireman, D., Guedes, D., Jr., W.M., Ferreira, R.: Achieving multi-level parallelism in filter-labeled stream programming model. In: The 37th International Conference on Parallel Processing (ICPP) (2008)
52. Teodoro, G., Hartley, T., Catalyurek, U., Ferreira, R.: Optimizing dataflow applications on heterogeneous environments. *Cluster Computing* **15**, 125–144 (2012). URL <http://dx.doi.org/10.1007/s10586-010-0151-6>
53. Teodoro, G., Hartley, T.D.R., Catalyurek, U., Ferreira, R.: Run-time optimizations for replicated dataflows on heterogeneous environments. In: Proc. of the 19th ACM International Symposium on High Performance Distributed Computing (HPDC) (2010)
54. Teodoro, G., Kurc, T.M., Pan, T., Cooper, L.A., Kong, J., Widener, P., Saltz, J.H.: Accelerating Large Scale Image Analyses on Parallel, CPU-GPU Equipped Systems. In: 26th IEEE International Parallel and Distributed Processing Symposium (IPDPS) (2012)
55. Teodoro, G., Sachetto, R., Sertel, O., Gurcan, M., Jr., W.M., Catalyurek, U., Ferreira, R.: Coordinating the use of GPU and CPU for improving performance of compute intensive applications. In: IEEE Cluster (2009)
56. Teodoro, G., Valle, E., Mariano, N., Torres, R., Meira Jr., W.: Adaptive parallel approximate similarity search for responsive multimedia retrieval. In: Proceedings of the 20th ACM international conference on Information and knowledge management, CIKM '11, pp. 495–504. ACM, New York, NY, USA (2011). DOI 10.1145/2063576.2063651
57. Tuytelaars, T., Mikolajczyk, K.: Local invariant feature detectors: a survey. *Found. Trends. Comput. Graph. Vis.* **3**, 177–280 (2008). DOI 10.1561/06000000017
58. Valle, E., Cord, M., Philipp-Foliguet, S.: Fast identification of visual documents using local descriptors. In: Proceeding of the eighth ACM symposium on Document engineering, DocEng '08, pp. 173–176. ACM (2008). DOI 10.1145/1410140.1410175
59. Valle, E., Cord, M., Philipp-Foliguet, S.: High-dimensional descriptor indexing for large multimedia databases. In: Proceeding of the 17th ACM conference on Information and knowledge management, CIKM '08, pp. 739–748. ACM, New York, NY, USA (2008). DOI 10.1145/1458082.1458181
60. Valle, E., Cord, M., Phillip-Foliguet, S., Gorisse, D.: Indexing personal image collections: A flexible, scalable solution. *IEEE Trans. Consumer Elect.* **56**, 1167–1175 (2010). DOI 10.1109/TCE.2010.5606242
61. Welsh, M., Culler, D., Brewer, E.: Seda: an architecture for well-conditioned, scalable internet services. *SIGOPS Oper. Syst. Rev.* **35**(5), 230–243 (2001). DOI 10.1145/502059.502057
62. Yiu, M.L., Mamoulis, N.: Multi-dimensional top-k dominating queries. *The VLDB Journal* **18**, 695–718 (2009). DOI 10.1007/s00778-008-0117-y
63. Yu, H., Rauchwerger, L.: Adaptive reduction parallelization techniques. In: Proc. of the 14th Int. Conf. on Supercomputing, ICS '00, pp. 66–77. ACM, New York, NY, USA (2000). DOI 10.1145/335231.335238
64. Zezula, P., Amato, G., Dohnal, V., Batko, M.: *Similarity Search: The Metric Space Approach*, 1st edn. Springer Publishing Company, Incorporated (2010)